Neurogenin 3 is essential for the proper specification of gastric enteroendocrine cells and the maintenance of gastric epithelial cell identity

Catherine S. Lee,[1] Nathalie Perreault,[1] John E. Brestelli, and Klaus H. Kaestner[2]

Department of Genetics, University of Pennsylvania School of Medicine, Philadelphia, Pennsylvania 19104, USA

The notch signaling pathway is essential for the endocrine cell fate in various tissues including the enteroendocrine system of the gastrointestinal tract. Enteroendocrine cells are one of the four major cell types found in the gastric epithelium of the glandular stomach. To understand the molecular basis of enteroendocrine cell development, we have used gene targeting in mouse embryonic stem cells to derive an *EGFP*-marked null allele of the bHLH transcription factor, *neurogenin 3* (*ngn3*). In *ngn3*$^{-/-}$ mice, glucagon secreting A-cells, somatostatin secreting D-cells, and gastrin secreting G-cells are absent from the epithelium of the glandular stomach, whereas the number of serotonin-expressing enterochromaffin (EC) cells is decreased dramatically. In addition, *ngn3*$^{-/-}$ mice display intestinal metaplasia of the gastric epithelium. Thus, *ngn3* is required for the differentiation of enteroendocrine cells in the stomach and the maintenance of gastric epithelial cell identity.

[*Key Words*: Basic-helix-loop-helix (bHLH) protein; *neurogenin 3* (*ngn3*); notch signaling; metaplasia; enteroendocrine cells; iFABP; *Muc 2*]

Received February 15, 2002; revised version accepted May 2, 2002.

The mouse stomach is divided into two domains, the proximal third, which is known as the forestomach and is lined with a keratinized squamous epithelium, and the distal two-thirds that make up the stomach proper, which is lined with a glandular epithelium containing four major cell types, that is, pit, parietal, zymogenic, and enteroendocrine cells (Lorenz and Gordon 1993; Gordon and Hermiston 1994). Endocrine cells produce peptide hormones that regulate various physiological functions (Skipper and Lewis 2000). The specification of endocrine cells from a population of precursor cells is thought to be in part mediated by the *Notch*-signaling pathway (Artavanis-Tsakonas et al. 1999). Upon activation by ligands such as *Delta* or *Jagged* on adjacent cells, the intracellular domain of the *Notch* receptor is cleaved and translocated to the nucleus with subsequent upregulation of downstream targets including the *Hairy/Enhancer of Split* (*HES*) genes. The HES proteins then inhibit the expression of several bHLH transcription factors including the *neurogenin* genes (Sommer et al. 1996; Artavanis-Tsakonas et al. 1999).

The bHLH transcription factors are instrumental in the determination of various cell fates including that of many endodermal endocrine cells. For example, gene targeting experiments in mice have shown that *Mash1* is required for endocrine cell differentiation in the lung (Borges et al. 1997), whereas loss of *Math1* leads to depletion of the secretory cell lineage in the intestine (Yang et al. 2001). Loss of *BETA2/NeuroD* results in diminished numbers of pancreatic α- and β-cells, as well as secretin- and cholecystokinin (CCK)-expressing cells of the gut (Naya et al. 1997), whereas deletion of *neurogenin 3* results in the absence of all four pancreatic endocrine cell types (Gradwohl et al. 2000). In addition, ablation of the repressor of bHLH gene expression, *Hes1*, leads to precocious and excessive differentiation of enteroendocrine cells in the gastrointestinal tract, underscoring the importance of the *Notch*-signaling pathway in the specification of enteroendocrine cells (Jensen et al. 2000). In this study, we have generated mice lacking *ngn3* and have analyzed the role of *ngn3* during gastric epithelial development. Using this model, we have uncovered an important role for *ngn3* in enteroendocrine cell differentiation and the maintenance of gastric epithelial cell identity.

[1]These authors contributed equally to this work.
[2]Corresponding author.
E-MAIL kaestner@mail.med.upenn.edu; FAX (215) 573-5892.
Article and publication are at http://www.genesdev.org/cgi/doi/10.1101/gad.985002.

Results

Derivation of ngn3–EGFP *mice*

To investigate the potential role of the bHLH transcription factor *ngn3* during stomach development, we have derived mice homozygous for a null mutation of this gene by homologous recombination in mouse embryonic stem (ES) cells. We constructed a targeting vector that replaces the entire coding region of *ngn3* with the enhanced green fluorescent protein (*EGFP*) gene (Fig. 1A). Of 200 stably transfected ES cell clones obtained after G418 selection, two were homologous recombinants as identified by PCR screening (Fig. 1B; data not shown). Germ-line chimeras and mice heterozygous for the *ngn3* mutation were obtained. Heterozygous animals of the original mixed background (129Sv × C57BL6) were crossed, and the offspring were genotyped by PCR (Fig. 1C). No gross differences were observed between heterozygous and wild-type animals in overall development, growth characteristics, and histology; therefore, mice of both genotypes were used as controls throughout this study.

Ngn3–EGFP *marks the enteroendocrine cell lineage of the glandular stomach*

During endocrine lineage development in the pancreas, *ngn3* is expressed transiently in endocrine precursor cells, but extinguished in fully differentiated cells (Gradwohl et al. 2000). To investigate the expression domain of *ngn3* in the stomach, we made use of our *ngn3–EGFP* allele to follow the expression of *ngn3* by green fluorescence. *Ngn3–EGFP* was located specifically in the glandular stomach, whereas no expression was detected in the squamous epithelium of the forestomach (Fig. 1F). The image of the *ngn3* heterozygous stomach shown in Figure 1F was obtained by imaging the entire organ on a confocal fluorescence microscope. Due to the low intensity of the *ngn3–EGFP* signal, the image was captured from multiple focal planes, thus giving the impression of a high density of enteroendocrine cells in the glandular stomach. To delineate the identity of these EGFP-positive cells, we examined the coexpression of the pan-endocrine marker, Chromogranin A, with EGFP in the stomach of heterozygous mice. In addition to multiple single-label EGFP-positive cells that presumably mark enteroendocrine precursor cells, we also observed numerous EGFP/Chromogranin A double-positive cells. The long half-life of EGFP thus allowed us to trace the fate of the *ngn3–EGFP*-positive endocrine precursors to their mature descendants. These data suggest that *ngn3–EGFP* marks the enteroendocrine lineage in the stomach (Fig. 1G).

Ngn3$^{-/-}$ *mice display a disorganized gastric mucosa*

Ngn3$^{-/-}$ mice derived previously are born alive with reduced size and experience 100% mortality by postnatal day 3 due to severe diabetes (Gradwohl et al. 2000). We observed similar abnormalities in our *ngn3*$^{-/-}$ mice (Fig. 1D), including the lack of the four endocrine cell types of the pancreas. However, in addition to this pancreatic phenotype, *ngn3*$^{-/-}$ mice also have previously undescribed abnormalities in other endodermally derived organs, including smaller stomachs (Fig. 1E). To further analyze the gastric phenotype of *ngn3*$^{-/-}$ mice, we examined gastric histology in 3-day-old control and *ngn3*$^{-/-}$ mice (Fig. 2A–H). We utilized Alcian blue staining to detect potential transformation of the gastric epithelium to intestinal cell types. Alcian blue stains acidic mucins that are normally found exclusively in the goblet cells of the small intestine and colon. Whereas the gastric mucosa of control mice contained no Alcian blue staining cells (Fig. 2C,E), a significant number of stained cells were found in the *ngn3*$^{-/-}$ gastric mucosa (Fig. 2D,F), suggesting regional intestinal metaplasia of the stomach. At higher magnification, we noticed that the Alcian blue positive cells in the *ngn3*$^{-/-}$ gastric epithelium are elongated, resembling the shape of a goblet cell (Fig. 2F). To assess whether these cells are goblet cells, we examined the ultrastructure of control and *ngn3*$^{-/-}$ stomachs by electron microscopy. As expected, no goblet cells were present in control stomachs (Fig. 2G), whereas goblet-like cells occurred frequently in the *ngn3*$^{-/-}$ stomach (Fig. 2H). These goblet cells appear immature, as they exhibit relatively few mucin-containing vesicles.

To support these findings on the molecular level, two intestine-specific markers, *Muc2* and iFABP, were analyzed for expression by RT–PCR, RNase protection assay, and immunohistochemistry. *Muc2* is normally expressed in goblet cells in the intestine (van Klinken et al. 1999; Longman et al. 2000), and iFABP is restricted to both absorptive enterocytes and goblet cells of the intestine (Sweetser et al. 1988). *Muc2* expression was detected in *ngn3*$^{-/-}$, but not in control stomachs as shown by RT–PCR (Fig. 3A) and RPA (Fig. 3B) analysis. As expected, no iFABP-positive cells were found in the gastric epithelium of controls (Fig. 3C), whereas iFABP expression was induced in the gastric mucosa of *ngn3*$^{-/-}$ mice (Fig. 3D). Quantification of iFABP-positive cells showed a 13-fold increase in the number of iFABP-expressing cells in the gastric epithelium of *ngn3*$^{-/-}$ mice compared with littermate controls (Fig. 3E). Taken together, data from histological and molecular analyses implicate *ngn3* in the maintenance of the gastric mucosal identity in the developing stomach, as its absence leads to regional intestinal metaplasia of the gastric epithelium.

Proliferation and apoptosis are normal in the gastric epithelium of Ngn$^{-/-}$ *mice*

The reduced size and expanded mucosal thickness of *ngn3*$^{-/-}$ stomachs prompted us to measure rates of proliferation and apoptosis in these mice using Ki67 and Caspase 3, respectively, as markers (Schluter et al. 1993; Yuan et al. 1993; Stennicke and Salvesen 1997). The pattern and numbers of proliferating cells stained by Ki67 were similar in the gastric mucosa of control and *ngn3*$^{-/-}$ mice (Fig. 4A,B). This suggests that the expanded gastric

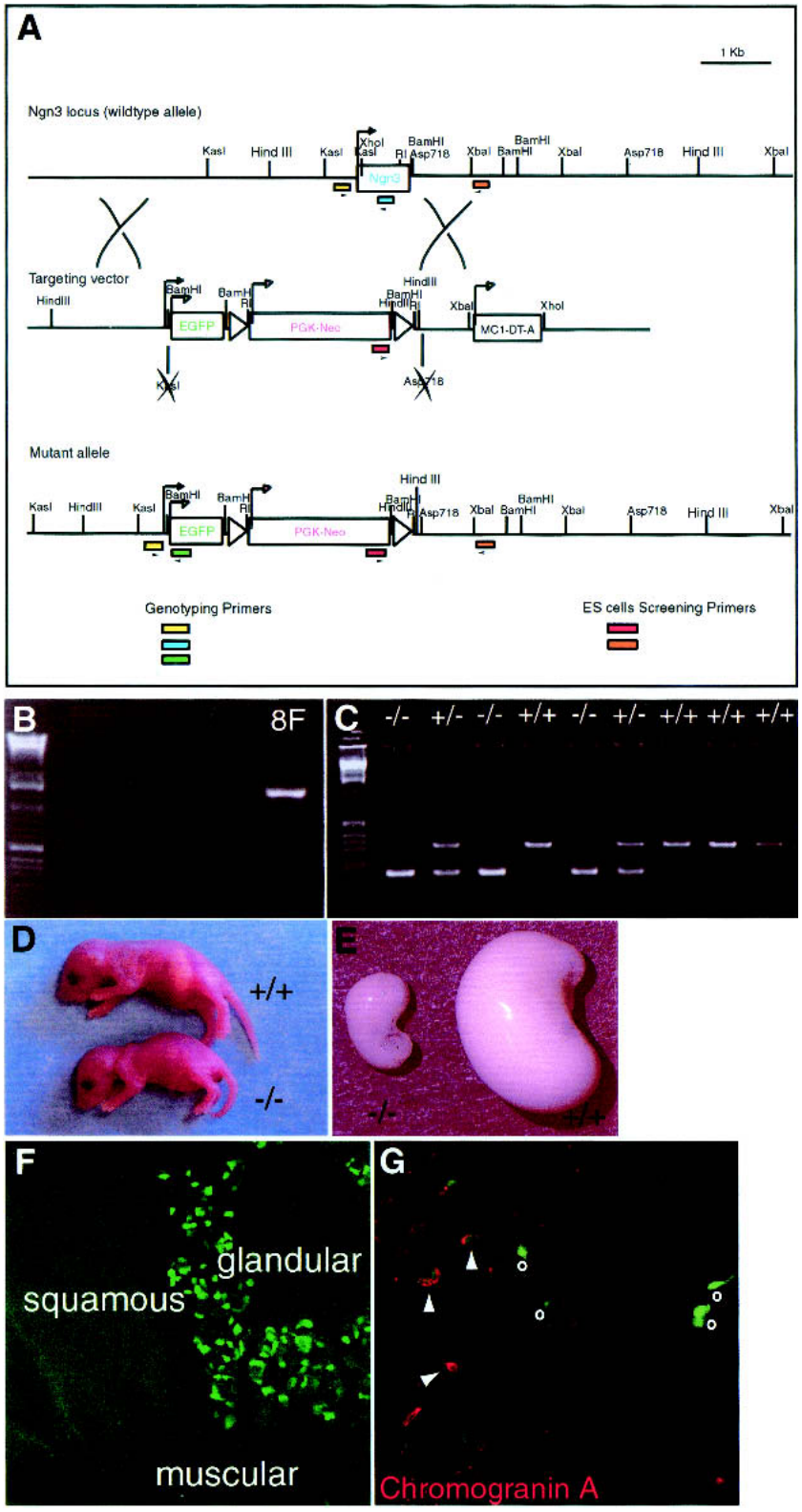

Figure 1. Targeting strategy for *ngn3* inactivation. (*A*) Gene structure of the *ngn3* locus (*top*). Targeting vector used for homologous recombination in ES cells (*middle*). Gene structure of the targeted allele (*bottom*). Not all of the restriction enzymes are depicted in the diagram. (*B*) An ES clone (8F) that has undergone homologous recombination was identified using ES screening primers (indicated by red and orange boxes in *A*). (*C*) Genotyping by PCR of a litter from an intercross of heterozygous mice. Three sets of genotyping primers (indicated by yellow, blue, and green boxes in *A*) were used to generate the wild-type (295 bp) and mutant (188 bp) allele bands. (*D*) Photograph of 3-day-old wild-type (*top*) and $ngn3^{-/-}$ mice (*bottom*) on a mixed 129Sv × C57BL6 background. $Ngn3^{-/-}$ animals were smaller, dehydrated, and diabetic. (*E*) Photograph of the stomachs of 3-day-old wild-type (*right*) and $ngn3^{-/-}$ mice (*left*). Note the smaller size of the $ngn3^{-/-}$ stomach. (*F*) Confocal images of EGFP expression in the P3 heterozygous animal. *ngn3–EGFP* expression is detected only in the glandular stomach. (*G*) *ngn3–EGFP* is expressed in the enteroendocrine precursor cells. Confocal image of heterozygous stomach stained using a Cy3-conjugated secondary antibody against Chromogranin A that allows simultaneous detection of Chromogranin A (red) and *ngn3* expression (green). Some cells expressed EGFP alone (indicated by o), whereas others were colabeled with both EGFP and Chromogranin A (indicated by arrowheads).

epithelium observed in $ngn3^{-/-}$ mice is not caused by increased proliferation. Next, we examined the possibility of altered programmed cell death in the $ngn3^{-/-}$mucosa by caspase 3 staining. As shown in Figure 4, C and D, we did not observe a significant difference in the number of apoptotic cells between control and $ngn3^{-/-}$ mice. Thus, it appears likely that the disorganization of the $ngn3^{-/-}$ mucosa causes the gastric epithelium to ap-

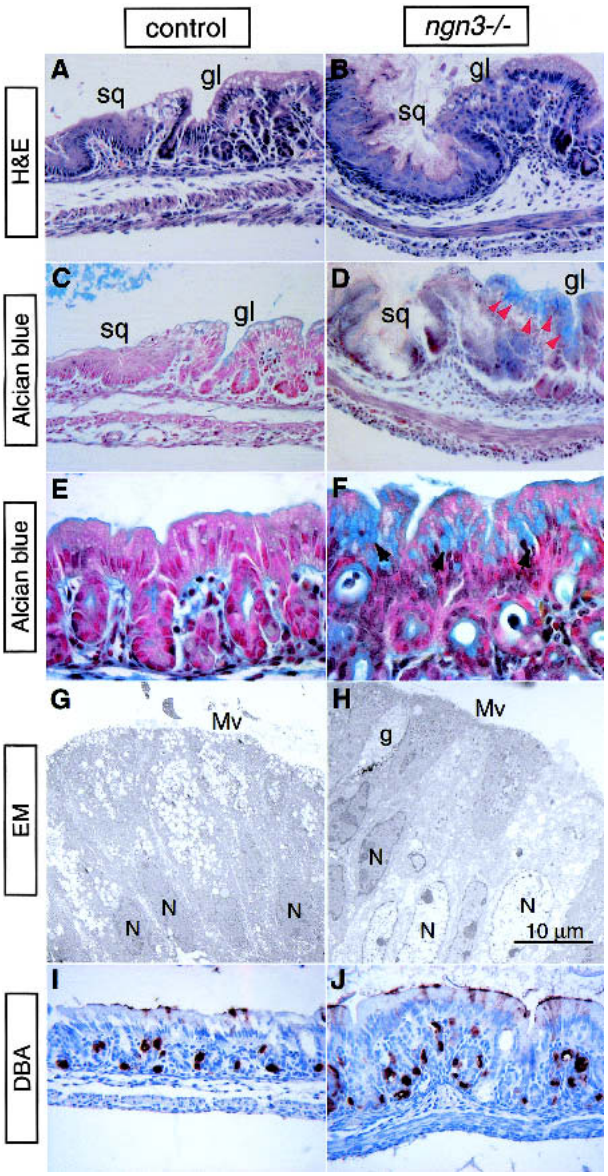

Figure 2. Abnormal stomach development in *ngn3*$^{-/-}$ mice. Paraffin sections of stomachs obtained from 3-day-old control (*A*,*C*,*E*,,*I*) and *ngn3*$^{-/-}$ mice (*B*,*D*,*F*,*J*) were stained with histological and lectin stains. Hematoxylin and eosin staining of control (*A*) and *ngn3*$^{-/-}$ (*B*) stomachs. Note increased diameter and disorganized appearance of the gastric epithelium in *ngn3*$^{-/-}$ mice. (*C*,*E*) Alcian blue, which detects acid mucins, normally does not stain the gastric epithelium, but detects ectopic acid mucins in the *ngn3*$^{-/-}$ mice (*D*,*F*, indicated by red and black arrowheads). Electron micrographs illustrate the ultrastructural features of the stomach. (*G*) An image of a control stomach showing normal epithelial morphology, whereas goblet-like cells were present in the *ngn3*$^{-/-}$ stomach (*H*). Control and *ngn3*$^{-/-}$ glandular epithelium were stained with *Dolichos biflorus* (DBA) lectin, which labels parietal cells, with horseradish peroxidase substrate (brown). The DBA staining shows no difference in the number and distribution of parietal cells between the control (*I*) and *ngn3*$^{-/-}$ gastric epithelium (*J*). Magnification for *A–D* and *I–J* is 400×, E–F is 600×, and *G–H* is 5000×. (sq) Squamous epithelium; (gl) glandular epithelium; (g) goblet cell; (Mv) microvilli; (N) nucleus.

pear thicker than that of the control stomach. Finally, it is possible that the smaller size of the stomach in the 3-day-old *ngn3*$^{-/-}$ mice is an indirect result of the abnormal metabolic status of these animals, as there was no difference in the fetal development of the organ when stomachs of control and *ngn3*$^{-/-}$ animals were compared at embryonic day 17.5 (data not shown).

Gastric enteroendocrine differentiation is impaired in ngn3$^{-/-}$ *mice*

To determine whether enteroendocrine cells are affected in the *ngn3*$^{-/-}$ stomach, expression of a general enteroendocrine cell marker, Chromogranin A, was examined by immunofluorescence. All major endocrine cell types express Chromogranin A in the stomach (Norlen et al. 2001). As shown in Figure 5, B and C, there were fewer Chromogranin A-positive cells in the *ngn3*$^{-/-}$ stomach than in the control. To distinguish the subtypes of enteroendocrine cells affected by the lack of *ngn3*, we utilized markers specific for A-, D-, G-, and EC-cells (Fig. 5A). Whereas cells expressing glucagon, somatostatin, and gastrin were found in the control stomach, none of these peptide hormones was detected in the gastric epithelium of *ngn3*$^{-/-}$ mice (Fig. 5F–K). In contrast, serotonin-positive cells were still present in the *ngn3*$^{-/-}$ stomach, but at reduced frequency (Fig. 5D–E; Fig. 6C). The expression of *BETA2/NeuroD*, a downstream target of *ngn3* (Huang et al. 2000), which plays an important role during endodermal endocrine cell differentiation, was absent in the *ngn3*$^{-/-}$ stomach as assessed by quantitative RT–PCR analysis (data not shown). This suggests that *ngn3* regulates the enteroendocrine lineage in the stomach through *BETA2/NeuroD*, similar to the transcription factor hierarchy that specifies pancreatic endocrine cells (Gradwohl et al. 2000).

Glucagon, somatostatin, and gastrin mRNAs are absent in the stomach of ngn3$^{-/-}$ *mice*

Although immunofluorescence is useful to investigate enteroendocrine cell differentiation, it is also crucial to determine the expression level of the marker genes quantitatively. Thus, we investigated glucagon, somatostatin, and gastrin mRNA levels in the control and *ngn3*$^{-/-}$ stomach by RT–PCR analysis. Consistent with what we have observed in our immunofluorescence studies, glucagon, somatostatin, and gastrin mRNA were completely absent in the *ngn3*$^{-/-}$ stomach, whereas these transcripts were detected in the control stomach (Fig. 6A). Interestingly, we have found a broad range of gastrin mRNA levels in the control stomachs, which might reflect small differences in the age or nutritional status of these animals.

In addition, we performed microarray expression profiling using various platforms with total RNA extracted from both control and *ngn3*$^{-/-}$ stomach. As shown in Figure 6B, the mRNA levels for proglucagon, somatostatin, and gastrin were decreased by 22-, 7-, and 14-fold,

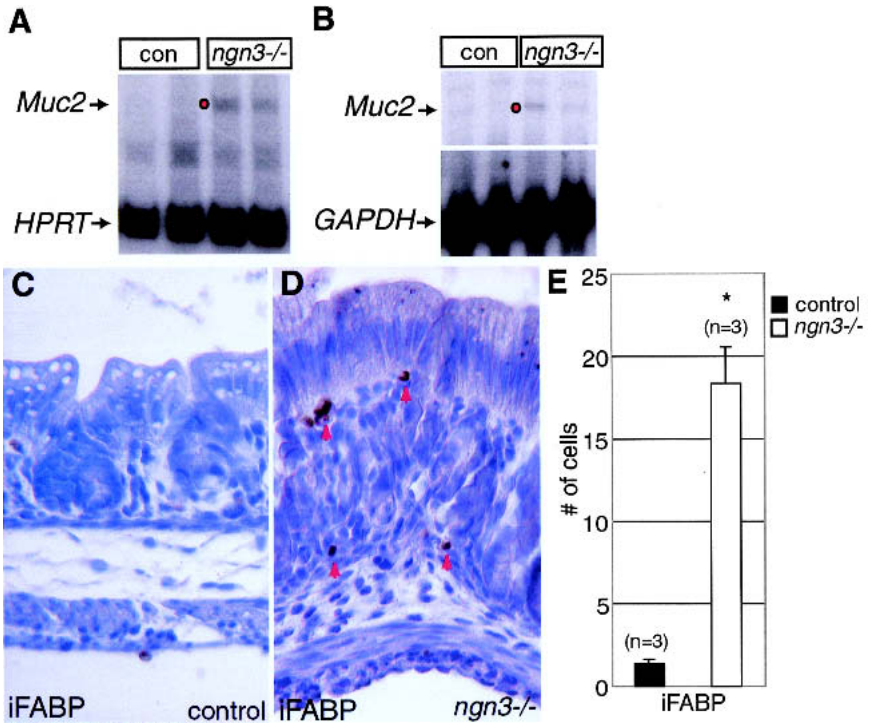

Figure 3. Up-regulation of intestine-specific gene expression in the stomach of *ngn3*$^{-/-}$ mice. *Muc2* mRNA–PCR and RNase protection assay (RPA) analysis. (*A*) RT–PCR analysis of total RNA isolated from whole stomach of control and *ngn3*$^{-/-}$ mice. *Muc2* expression (215 bp) is detected in the *ngn3*$^{-/-}$ stomach ($n = 2$), whereas no *Muc2* expression is found in the control ($n = 2$). Hypoxanthine phosphoribosyl transferase (*HPRT*) was used as a loading control (130 bp). (*B*) RPA analysis of 10 µg of total RNA from 3-day-old control ($n = 2$) and *ngn3*$^{-/-}$ stomach ($n = 2$). Glyceraldehyde phosphate dehydrogenase (*GAPDH*) served as loading control. *Muc2* mRNA was again seen in *ngn3*$^{-/-}$ stomach. Notably, the *ngn3*$^{-/-}$ stomach that showed higher expression of *Muc2* by RT–PCR analysis also showed higher expression of *Muc2* by RPA (indicated by dot in both *A* and *B*). (*C–D*) Immunohistochemical detection of intestinal fatty acid-binding protein (iFABP) in *ngn3*$^{-/-}$ stomach. Paraffin sections from 3-day-old control and *ngn3*$^{-/-}$ glandular stomach were stained with an antiserum specific to iFABP (indicated by red arrowheads). iFABP is expressed by the misspecified gastric epithelial cells in *ngn3*$^{-/-}$ mice (*D*), but was not detected in controls (*C*). Magnification, 400×. (*E*) iFABP-positive cells were counted from control ($n = 3$) and *ngn3*$^{-/-}$ stomachs ($n = 3$). Y-axis represents the iFABP-positive cell counts. (*) $P < 0.02$ by two-tailed Student's *t*-test.

respectively, in *ngn3*$^{-/-}$ stomachs, consistent with our RT–PCR results. In contrast, the intestinal markers, Trefoil factor 3 (TFF3; Mashimo et al. 1995), and iFABP were found to be increased by 18- and 3-fold, respectively in the *ngn3*$^{-/-}$ stomachs, respectively, confirming the presence of regional intestinal metaplasia of the stomach in *ngn3*$^{-/-}$ mice described above. The expression of the $H^{+/K+}$ ATPase, a marker for parietal cells, showed no difference between the control and *ngn3*$^{-/-}$ stomachs, again confirming our histological findings (see below).

As multiple attempts at establishing an RT–PCR protocol for serotonin were unsuccessful, and as serotonin is

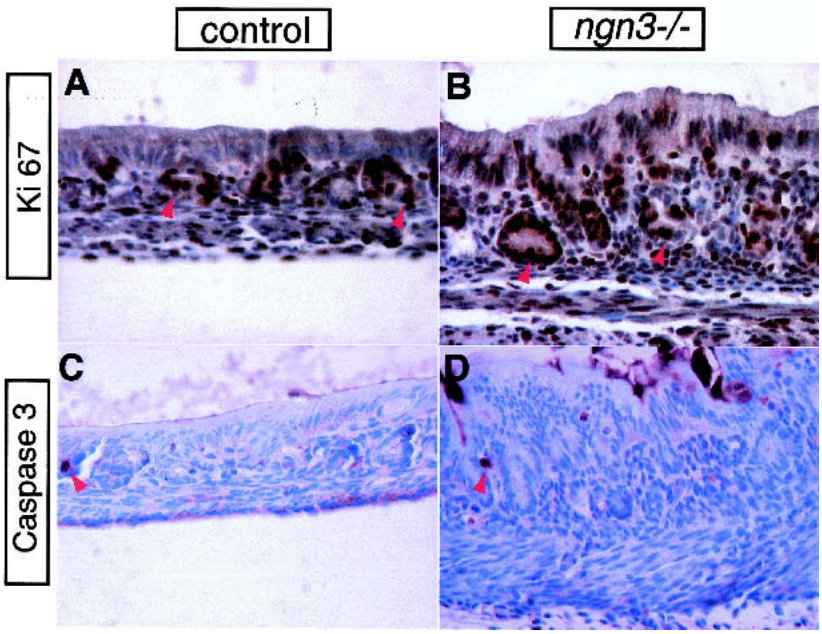

Figure 4. *Ngn3*$^{-/-}$ gastric mucosa does not display abnormal cell proliferation or programmed cell death. Proliferating cells stained by Ki67 are found in the gastric glands (arrowheads), mesenchymal, and muscular layers of control (*A*) and *ngn3*$^{-/-}$ stomach (*B*). There was no significant difference in the number or localization of proliferating cells between the mutant and control groups. Caspase 3 immunostaining (arrowheads) showed no significant changes in numbers of apoptotic cells between control (*C*) and *ngn3*$^{-/-}$ (*D* stomachs). Magnification, 400×.

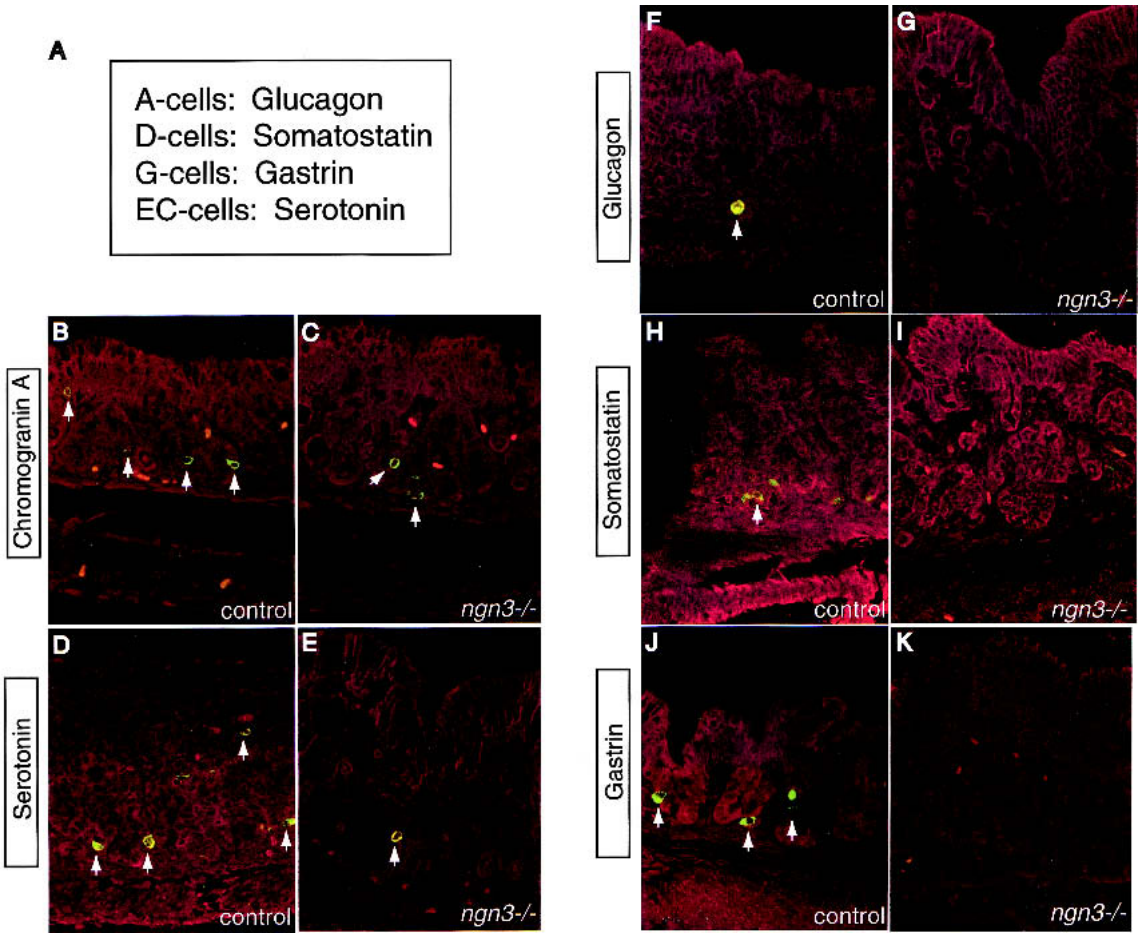

Figure 5. *Ngn3* is required for the differentiation of enteroendocrine cells in the gastric epithelium. (*A*) Classification of enteroendocrine cells by their main secretory products. Immunofluorescence was performed on paraffin sections from 2–3-day-old control (*B*,*D*,*F*,*H*,*J*) and *ngn3*$^{-/-}$ (*C*,*E*,*G*,*I*,*K*) glandular stomach. Immunostained cells are labeled in green for the enteroendocrine cell-specific antigen indicated at *left* (labeled by white arrows), and images were captured by confocal microscopy. Evan's blue was used as counterstain for the tissues and is visualized in red in all sections (Beaulieu 1997). (*B*) Chromogranin A, a general endocrine cell maker, labels all subtypes of enteroendocrine cells in the gastric epithelium of control mice. (*C*) The number of Chromogranin A-expressing cells is reduced in the *ngn3*$^{-/-}$ gastric epithelium. (*D*) An enterochromaffin (EC) cell-specific marker, serotonin, is normally expressed by the EC-cells in the control stomach. (*E*) The number of serotonin-positive cells is reduced in the *ngn3*$^{-/-}$ stomach. (*F*) An A-cell-specific enteroendocrine cell marker, glucagon, is normally present in the gastric epithelium of control stomach. (*G*) No glucagon-positive cells are found in the *ngn3*$^{-/-}$ gastric epithelium. (*H*) Somatostatin, a D-cell-specific enteroendocrine cell maker, is found in the control gastric epithelium. (*I*) Somatostatin expression is not present in the *ngn3*$^{-/-}$ stomach. (*J*) Gastrin expression is found in the G-cells of control gastric epithelium. (*K*) No gastrin-positive cells are found in the *ngn3*$^{-/-}$ gastric epithelium. Magnification, 400×.

not included on the microarrays used for our study, we quantified the level of serotonin expression by counting cells that are immunostained with serotonin antibody from both control and *ngn3*$^{-/-}$ stomachs. We observed an overall sixfold decrease in the numbers of serotonin-positive cells in the *ngn3*$^{-/-}$ stomachs when compared with controls (Fig. 6C).

Parietal and mucous cells are not affected in the ngn3$^{-/-}$ *stomach*

In addition to enteroendocrine cells, other cell types such as zymogenic cells, mucin-producing pit cells, and parietal cells are also present in the gastric mucosa (Gordon and Hermiston 1994). As it has been shown that gastrin deficiency leads to a decrease in the number of parietal cells and an increase in mucous neck cell number in gastrin-deficient mice (Koh et al. 1997), we sought to determine whether these lineages were also affected by the loss of gastrin expression observed in the stomach of *ngn3*-deficient mice (Fig. 5K). For this purpose, we utilized lectin staining, which is a sensitive tool for defining the differentiation program of gut epithelial cell lineages. Immunohistochemistry with DBA and AAA, which label parietal and mucous cells, respectively (Falk et al. 1994), revealed no differences between the control and *ngn3*$^{-/-}$ stomachs (Fig. 2I–J; data not shown). These data indicate that the gastric parietal and mucous cell

lineages are not regulated by *ngn3* and are not affected by the lack of gastrin in the stomach. The apparent discrepancy in the observations in gastrin-deficient mice cited above might be explained by the difference in the age of the animals investigated. Due to the early lethality of *ngn3*$^{-/-}$ mice, we had to limit our analysis to postnatal day 3, whereas the phenotype of gastrin null mice is only apparent in adult mice (7–8 wk old) (Koh et al. 1997).

Discussion

Models for the role of ngn3 *during gastric enteroendocrine cell differentiation*

Our analysis in *ngn3*$^{-/-}$ mice suggests the existence of both *ngn3*-dependent and independent enteroendocrine cell lineages. We propose two models to illustrate how *ngn3* might specify gastric enteroendocrine development (Fig. 7). The first model suggests that *ngn3* is needed initially for the proliferation of all endocrine cells, and subsequently required for the terminal differentiation of A-, D-, and G-cells, but not EC-cells (Fig. 7A). Thus, *ngn3* deficiency leads to a smaller pool of enteroendocrine precursors from which EC-cells can differentiate, resulting in the observed reduction in the frequency of this cell type. The second model suggests that *ngn3* is absolutely required for the specification of A-, D-, and G-cells, but not EC-cells, because the specification of EC-cells can also be orchestrated by factor X (Fig. 7B). Factor X could be regulated by effectors in the *Notch*-signaling pathway or by factors in other signaling pathways. Other *neurogenin* family members such as *ngn1* and *ngn2* are potential candidates for factor X that might also be involved in governing enteroendocrine cell specification. In conclusion, we have shown that *ngn3* is essential for the specification of enteroendocrine cells in the stomach and for the maintenance of gastric epithelial cell identity.

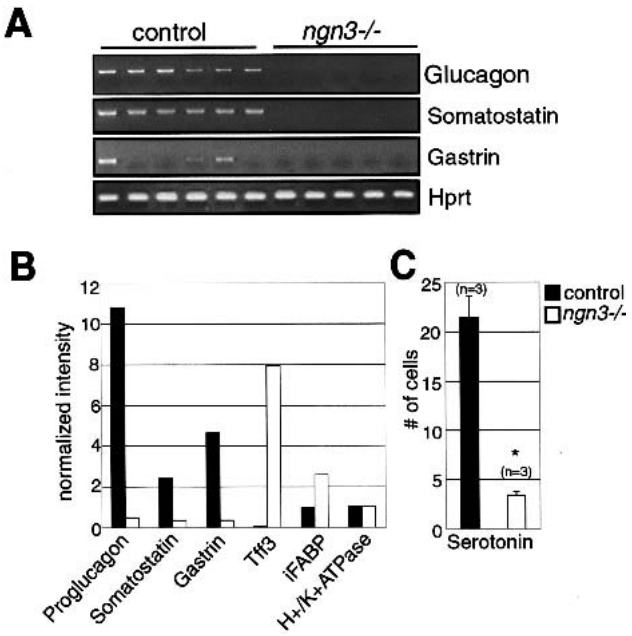

Figure 6. Analysis of mRNA levels of secretory products of enteroendocrine cells and gastrointestinal marker genes. (*A*) Glucagon, Somatostatin, and Gastrin mRNA are absent in 2–3-day-old *ngn3*$^{-/-}$ stomachs. RT–PCR analysis was performed using the primers indicated and the products separated on 1.5% ethidium bromide-stained agarose gels. Hprt was used as an internal control. $n = 6$ for controls and $n = 5$ for *ngn3*$^{-/-}$ stomachs. (*B*) Summary of genes with altered expression levels identified by microarray analysis. Y-axis shows the normalized intensity levels and X-axis shows the various genes examined. $n = 2$ for controls and $n = 3$ for *ngn3*$^{-/-}$ stomachs. (*C*) Quantification of serotonin-positive cells. Ten sections from each stomach were counted for both control and *ngn3*$^{-/-}$ animals. $n = 3$ for both control (black bar) and *ngn3*$^{-/-}$ stomachs (white bar). Y-axis represents the serotonin-positive cell counts. Serotonin-positive cells were decreased sixfold in the *ngn3*$^{-/-}$ stomachs. (*) $P < 0.02$ by two-tailed Student's *t*-test.

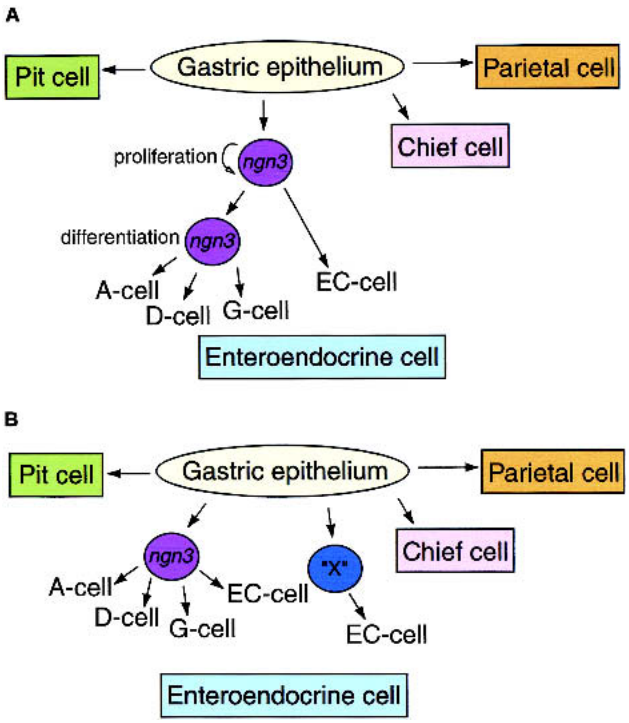

Figure 7. Two models for the proposed role of *ngn3* during enteroendocrine cell differentiation in the gastric epithelium. (*A*) *Ngn3* is needed for the proliferation of all enteroendocrine cells, but only required for the differentiation of A-, D-, and G-cells. EC-cells can differentiate in an *ngn3*-independent pathway, but their number is reduced in *ngn3*$^{-/-}$; mice as the total pool of enteroendocrine precursor cells is reduced. (*B*) *ngn3* is absolutely required for the differentiation of A-, D-, and G-cells. However, differentiation of the EC-cells can occur from either the *ngn3* lineage or another pathway regulated by an unidentified factor X.

Materials and methods

Derivation of the ngn3–EGFP *allele*

Primers specific to the mouse *ngn3* gene were used to screen a 129 SvEv mouse BAC (bacterial artificial chromosome) library

(Research Genetics). Three BACs containing the *ngn3* gene were identified and an 8-kb *Xba*I fragment of the final *ngn3* BAC was subcloned into pBluescript (Stratagene) (*ngn3xlx8.0*) and used for the construction of the targeting vector. Sequencing confirmed that the entire 642-bp *ngn3*-coding region was contained in *ngn3xlx8.0*. Furthermore, *ngn3xlx8.0* also contains a 6.4-kb 5′ flanking sequence and 948 bp of 3′UTR. The *ngn3*-coding region was replaced by the EGFP cDNA and a loxP-pgk-neomycin-loxP resistance cassette. The negative selectable marker Diphtheria Toxin A was cloned outside of the 3′ homology of *ngn3* to enhance the targeting frequency in ES cells. The targeting scheme is detailed in Figure 1A. The targeting vector was linearized with *Xho*I and 20 µg of DNA was electroporated into 10^7 TL1 embryonic stem cells (Labosky et al. 1997). Stably transfected cells were isolated after selection in 350 µg/mL G418 (GIBCO), and 200 clones were screened for homologous recombinants by PCR using the following primers: ES cell screening primer 1, 5′-ATAGCGTTGGCTACCCGTGAT-3′; ES cell screening primer 2, 5′-AGTCTCCCCTTGCTCCTCT CC-3′.

PCR reactions were carried out (95°C for 5 min, 32 cycles of 95°C for 45 sec, 60°C for 45 sec, 72°C for 2.5 min, and 72°C for 5 min) in a buffer containing 1.5 mM $MgCl_2$. The homologously recombined clones produced a band of 1.5 kb. ES cells from the correctly targeted clones were injected into blastocysts derived from C57BL/6 mice. Blastocysts were transferred to pseudopregnant females and chimeric offspring were identified by the presence of agouti hair. Chimeric males were mated to C57BL/6 females to obtain ES-derived offspring that were analyzed by PCR of tail DNA to identify the heterozygous ($ngn3^{-/-}$) mice. Embryos and mice were also genotyped by PCR using genotyping primers as follows: *ngn3*-1, 5′-ATACTCTGGTCCCCC GTG-3′; *ngn3*-2, 5′-TGTTTGCTGAGTGCCAACTC-3′; and EGFP, 5′-GAACTTGTGGCCGTTTACGT-3′. PCR reactions were as follows: 95° C for 5 min, 32 cycles of 95°C for 45 sec, 60°C for 45 sec, 72°C for 90 sec, and 72°C for 5 min, in a buffer containing 1.5 mM $MgCl_2$.

Histology

Tissues were fixed in 4% paraformaldehyde overnight at 4°C, embedded in paraffin, cut to 6-µm sections, and applied to Probe-on Plus slides (Fisher Scientific). For Alcian blue staining, tissues were deparaffinized in xylene, rehydrated, and placed in 3% acetic acid for 3 min and then incubated in 1% Alcian blue in 3% acetic acid (pH 2.5) for 30 min and washed in water. The slides were incubated in 0.1% nuclear fast red for 5 min as a counterstain, washed in water, dehydrated, and mounted with Cytoseal. For hematoxylin and eosin staining, tissues were incubated after rehydration in hematoxylin for 2.5 min, rinsed in water, dipped quickly in 0.5% acid alcohol, and washed in water. Tissues were then immersed in 0.2% $NaHCO_3$, rinsed in water, dipped in eosin for 15 sec and briefly rinsed in water before dehydration and mounting.

Electron microscopy

Tissues were fixed overnight in 2% glutaraldehyde in 0.1 M sodium cacodylate (pH 7.4) at 4°C. Sections were prepared following the standard protocol (Smith et al. 1985). Briefly, tissues were rinsed with 0.1M Sodium cacodylate, post fixed with 2% osmium tetroxide in 0.1 M sodium cacodylate and washed at 4°C. Tissues were stained with 2% aqueous uranyl acetate, dehydrated in graded alcohol, and embedded in Embed 812 resin (Electron Microscopy Sciences). Sections 7×10^{-8} m thick were cut using a Leica Ultracut microtome and mounted on 200 mesh thin bar copper grids, stained in 7% aqueous uranyl acetate, and counterstained in bismuth subnitrite. Digital images were collected on a JEOL JEM 1010 equipped with a Hamamatsu CCD camera and AMT 12-HR imaging software.

RNA analysis

Total RNA from postnatal stomach was isolated after homogenization and processed using the Totally RNA extraction kit (Ambion). RNase protection analysis was carried out using 10 µg of total RNA and the RPA II kit (Ambion) following the manufacturer's protocol. The probes used were *Muc2* (Silberg et al. 2001) and *GAPDH* (Ambion). RT–PCR analysis was performed as described previously (Wilson and Melton 1994; Duncan et al. 1997). To determine conditions for quantitative analysis, cDNA samples were diluted serially, and each primer pair was tested for exponential amplification by modifying PCR cycle number and quantifying the signal using PhosphorImager (Molecular Dynamics) analysis. PCR conditions were as follows: one cycle of 94°C, 3 min; 26 cycles of 94°C, 45 sec; 60°C, 45 sec; 72°C, 90 sec; one cycle of 72°C, 5 min in a buffer containing 1.5 mM $MgCl_2$. The following forward and reverse primers were used for specific amplification (size in basepairs):*Muc2* (215 bp), 5′-CATTTCTTGGGGCAGAGTGAG-3′ 5′-GAAT GTGAGAGGCTGCTGACC-3′; *Hprt* (130 bp), 5′-GGCCATC TGCCTAGTAAAGCT-3′ 5′-GCTGGCCTATAGGCTCATAGT-3′; *Proglucagon* (330 bp), 5′-GCACATTCACCAGCGACTACA-3′ 5′-CTGGTGGCAAGATTGTCCAGA-3′; *Somatostatin* (444 bp), 5′-GCTGAAGAAGACGCTACCGAA-3′ 5′-TGCAGGGTCAAGTT GAGCATC-3′; *Gastrin* (165 bp), 5′-GACCAATGAGGACCTG GAACA-3′ 5′-AAAGTCCATCCATCCGTAGGC-3′.

Immunofluorescence and immunohistochemistry

For immunofluorescence, tissues were fixed, sectioned, and processed as described above. Slides used for Chromogranin A were subjected to microwave antigen retrieval by boiling for 6 min in a 10-mM citric acid buffer (pH 6.0) and allowed to cool for 10 min at room temperature . All slides were washed in PBS, then blocked with protein blocking reagent (Immunotech) for 20 min at room temperature. The primary antibodies were diluted in PBS containing 0.1% BSA and 0.2% Triton X-100 (PBT) unless noted otherwise, and incubated with the sections overnight at 4°C. Slides were washed in PBS, then incubated with the appropriate secondary antibodies diluted in PBT for 2 h at room temperature. Slides were washed in PBS. To counterstain the tissues, slides were dipped in 0.01% Evan's Blue solution for 20 sec, rinsed in PBS, mounted, and examined using confocal microscopy (Leica). The following antibodies were used at the indicated dilutions for immunofluorescence: rabbit anti-Somatostatin (1:50 in Antibody Diluent Solution; Zymed), rabbit anti-Serotonin (1:50 in Antibody Diluent; Zymed), rabbit anti-Glucagon (Zymed), rabbit anti-Chromogranin A (1:3000; Diasorin), rabbit anti-GASP {Gastrin} (1:100; BMB), and FITC-conjugated donkey anti-rabbit IgG (1:50; Jackson).

For immunohistochemistry, tissues were fixed and processed as described above, and quenched in 2.25% hydrogen peroxide at room temperature for 20 min. Slides were blocked with Avidin D blocking reagent (Vector) and Biotin blocking reagent (Vector) for 15 min at room temperature with a quick rinse of PBS in between. All slides were blocked with protein-blocking reagent (Immunotech) for 20 min at room temperature. The primary antibodies were diluted in PBT and incubated overnight at 4°C. Slides were washed in PBS and incubated with goat anti-rabbit (1:200; Vector Laboratories) for 30 min at 37°C. Slides

were rinsed with PBS and incubated with HRP-conjugated ABC reagent (Vector Elite kit) for 30 min at 37°C. Slides were washed and colors were developed using a DAB substrate kit (Vector Laboratories). Slides for Ki67 immunohistochemistry were microwaved for antigen retrieval (see above). The following antibodies were used at the indicated dilutions for immunohistochemistry: rabbit anti-iFABP (1:2500; gift from J. Gordon, Washington University, St. Louis, MO), rabbit anti-human/mouse caspase 3 (activated) (1:750; R&D Systems), rabbit anti-Ki67 (1:5000; Novacastra), biotinylated-anti-rabbit IgG (1:200; Vector), and biotinylated-DBA lectin (1:20; EY Laboratories). Ki67 and Caspase 3-labeled nuclei were counted manually in a blinded fashion and care was taken only to evaluate gastric mucosa.

Whole-mount immunostaining

Milk was removed from the stomach and the tissue fixed in 4% PFA at room temperature for 30 min. Tissues were washed in PBS/0.1% TritonX (PT) for 30 min at room temperature, then blocked in PT/5%BSA at 4°C overnight. Rabbit anti-Chromogranin A (Diasorin) was added at 1:500 and incubated overnight at 4°C. Tissues were washed in PT/1%BSA for 1.5 h and Goat anti-Rabbit-Cy3 was added at 1:200 in PT/5%BSA for 1.5 h. Tissues were washed in PBS and mounted in PBS/50% glycerol for confocal microscopy (Pepling and Spradling 1998).

Microarray analysis

RNA samples were extracted as described above. cDNA was reverse transcribed and fluorescently labeled from 2 μg of total RNA using Cy3 dendrimers (Genisphere) from control ($n = 2$) and mutant ($n = 3$) stomachs. Common controls were pooled from the controls and mutants and labeled with Cy5 dendrimers. These probes were hybridized to the PancChip2 (Scearce et al. 2002) plus 6912 mouse 70-mer oligonucleotides (Operon) at 45°C according to the Genisphere protocol. A Genepix Scanner was used to scan the slides and the signals were quantified using the Genepix software (Axon). Concurrently, 10 μg of total RNA from control ($n = 2$) and mutant ($n = 3$) stomach were used to screen the Affymetrix MG_U74A version 1 chip. Data were acquired and analyzed according the Affymetrix protocol. Global normalization was used to obtain the normalized intensity levels.

Acknowledgments

We thank Drs. L.E. Greenbaum, D.G. Silberg, D. Stoffers, J.P. Katz, and F. Boudreau for insightful discussions and critical reading of the manuscript. We gratefully acknowledge the assistance of Dr. G. Swain, Sara McNally, and the members of the Morphology Core at the University of Pennsylvania, Drs. D. Baldwin and J. Wang in the Penn Microarray Facility, and Dr. Shah and the members of the Biomedical Imaging Core Laboratory. We thank Dr. Brian Calvi for the help with confocal microscopy, Kathleen O'Shea for the care of mouse colony, Dr. Jonathan P. Katz for the Muc2 primers, Bree Goldstein for technical assistance, and Dr. Marie Scearce for help with microarray analysis. Our studies were facilitated by the University of Pennsylvania Diabetes Center (P30-DK19525) and the Penn Center for Molecular Studies in Digestive and Liver Disease (P30-DK50306). This work was supported by the NIDDK (RO1 DK55342 and RO1 DK53839). C.S.L. is supported by the NIDDK (NRSA F32 DK61226–01). N.P. is supported by National Science and Engineering Research Council of Canada postdoctoral fellowship (BP-220106–1999).

The publication costs of this article were defrayed in part by payment of page charges. This article must therefore be hereby marked "advertisement" in accordance with 18 USC section 1734 solely to indicate this fact.

References

Artavanis-Tsakonas, S., Rand, M.D., and Lake, R.J. 1999. Notch signaling: Cell fate control and signal integration in development. *Science* **284:** 770–776.

Beaulieu, J.F. 1997. Extracellular matrix components and integrins in relationship to human intestinal epithelial cell differentiation. *Prog. Histochem. Cytochem.* **31:** 1–78.

Borges, M., Linnoila, R.I., van de Velde, H.J., Chen, H., Nelkin, B.D., Mabry, M., Baylin, S.B., and Ball, D.W. 1997. An achaete-scute homologue essential for neuroendocrine differentiation in the lung. *Nature* **386:** 852–855.

Duncan, S.A., Nagy, A., and Chan, W. 1997. Murine gastrulation requires HNF-4 regulated gene expression in the visceral endoderm: Tetraploid rescue of Hnf-4(–/–) embryos. *Development* **124:** 279–287.

Falk, P., Roth, K.A., and Gordon, J.I. 1994. Lectins are sensitive tools for defining the differentiation programs of mouse gut epithelial cell lineages. *Am. J. Physiol.* **266:** G987–G1003.

Gordon, J.I. and Hermiston, M.L. 1994. Differentiation and self-renewal in the mouse gastrointestinal epithelium. *Curr. Opin. Cell. Biol.* **6:** 795–803.

Gradwohl, G., Dierich, A., LeMeur, M., and Guillemot, F. 2000. neurogenin3 is required for the development of the four endocrine cell lineages of the pancreas. *Proc. Natl. Acad. Sci.* **97:** 1607–1611.

Huang, H.P., Liu, M., El-Hodiri, H.M., Chu, K., Jamrich, M., and Tsai, M.J. 2000. Regulation of the pancreatic islet-specific gene BETA2 (neuroD) by neurogenin 3. *Mol. Cell. Biol.* **20:** 3292–3307.

Jensen, J., Pedersen, E.E., Galante, P., Hald, J., Heller, R.S., Ishibashi, M., Kageyama, R., Guillemot, F., Serup, P., and Madsen, O.D. 2000. Control of endodermal endocrine development by Hes-1. *Nat. Genet.* **24:** 36–44.

Koh, T.J., Goldenring, J.R., Ito, S., Mashimo, H., Kopin, A.S., Varro, A., Dockray, G.J., and Wang, T.C. 1997. Gastrin deficiency results in altered gastric differentiation and decreased colonic proliferation in mice. *Gastroenterology* **113:** 1015–1025.

Labosky, P.A., Winnier, G.E., Jetton, T.L., Hargett, L., Ryan, A.K., Rosenfeld, M.G., Parlow, A.F., and Hogan, B.L. 1997. The winged helix gene, Mf3, is required for normal development of the diencephalon and midbrain, postnatal growth and the milk-ejection reflex. *Development* **124:** 1263–1274.

Longman, R.J., Douthwaite, J., Sylvester, P.A., Poulsom, R., Corfield, A.P., Thomas, M.G., and Wright, N.A. 2000. Coordinated localisation of mucins and trefoil peptides in the ulcer associated cell lineage and the gastrointestinal mucosa. *Gut* **47:** 792–800.

Lorenz, R.G. and Gordon, J.I. 1993. Use of transgenic mice to study regulation of gene expression in the parietal cell lineage of gastric units. *J. Biol. Chem.* **268:** 26559–26570.

Mashimo, H., Podolsky, D.K., and Fishman, M.C. 1995. Structure and expression of murine intestinal trefoil factor: High evolutionary conservation and postnatal expression. *Biochem. Biophys. Res. Commun.* **210:** 31–37.

Naya, F.J., Huang, H.P., Qiu, Y., Mutoh, H., DeMayo, F.J., Leiter, A.B., and Tsai, M.J. 1997. Diabetes, defective pancreatic morphogenesis, and abnormal enteroendocrine differentiation in BETA2/neuroD-deficient mice. *Genes & Dev.*

11: 2323–2334.
Norlen, P., Curry, W.J., Bjorkqvist, M., Maule, A., Cunningham, R.T., Hogg, R.B., Harriott, P., Johnston, C.F., Hutton, J.C., and Hakanson, R. 2001. Cell-specific processing of chromogranin A in endocrine cells of the rat stomach. *J. Histochem. Cytochem.* **49:** 9–18.
Pepling, M.E. and Spradling, A.C. 1998. Female mouse germ cells form synchronously dividing cysts. *Development* **125:** 3323–3328.
Scearce, L.M., Brestelli, J., McWeeney, S.K., Lee, C.S., Mazzarelli, J., Pinney, D.F., Pizarro, A., Stoeckert, C.J., Clifton, S., Permutt, M.A., et al. 2002. Functional genomics of the endocrine pancreas: The pancreas clone set and PancChip, new resources for diabetes research. *Diabetes* (in press).
Schluter, C., Duchrow, M., Wohlenberg, C., Becker, M.H., Key, G., Flad, H.D., and Gerdes, J. 1993. The cell proliferation-associated antigen of antibody Ki-67: A very large, ubiquitous nuclear protein with numerous repeated elements, representing a new kind of cell cycle-maintaining proteins. *J. Cell. Biol.* **123:** 513–522.
Silberg, D.G., Sullivan, J., Kang, E., Swain, G.P., Moffett, J., Sund, N.J., Sackett, S.D., and Kaestner, K.H. 2001. Cdx2 ectopic expression induces gastric intestinal metaplasia in transgenic mice. *Gastroenterology* **122:** 689–696.
Skipper, M. and Lewis, J. 2000. Getting to the guts of enteroendocrine differentiation. *Nat.Genet.* **24:** 3–4.
Smith, R.M., Cobb, M.H., Rosen, O.M., and Jarett, L. 1985. Ultrastructural analysis of the organization and distribution of insulin receptors on the surface of 3T3-L1 adipocytes: Rapid microaggregation and migration of occupied receptors. *J. Cell. Physiol.* **123:** 167–179.
Sommer, L., Ma, Q., and Anderson, D.J. 1996. neurogenins, a novel family of atonal-related bHLH transcription factors, are putative mammalian neuronal determination genes that reveal progenitor cell heterogeneity in the developing CNS and PNS. *Mol. Cell. Neurosci.* **8:** 221–241.
Stennicke, H.R. and Salvesen, G.S. 1997. Biochemical characteristics of caspases-3, -6, -7, and -8. *J. Biol. Chem.* **272:** 25719–25723.
Sweetser, D.A., Hauft, S.M., Hoppe, P.C., Birkenmeier, E.H., and Gordon, J.I. 1988. Transgenic mice containing intestinal fatty acid-binding protein-human growth hormone fusion genes exhibit correct regional and cell-specific expression of the reporter gene in their small intestine. *Proc. Natl. Acad. Sci.* **85:** 9611–9615.
van Klinken, B.J., Einerhand, A.W., Duits, L.A., Makkink, M.K., Tytgat, K.M., Renes, I.B., Verburg, M., Buller, H.A., and Dekker, J. 1999. Gastrointestinal expression and partial cDNA cloning of murine Muc2. *Am. J. Physiol.* **276:** G115–G124.
Wilson, P.A. and Melton, D.A. 1994. Mesodermal patterning by an inducer gradient depends on secondary cell-cell communication. *Curr. Biol.* **4:** 676–686.
Yang, Q., Bermingham, N.A., Finegold, M.J., and Zoghbi, H.Y. 2001. Requirement of math1 for secretory cell lineage commitment in the mouse intestine. *Science* **294:** 2155–2158.
Yuan, J., Shaham, S., Ledoux, S., Ellis H.M., and Horvitz, H.R. 1993. The *C. elegans* cell death gene ced-3 encodes a protein similar to mammalian interleukin-1 β-converting enzyme. *Cell* **75:** 641–652.